

See discussions, stats, and author profiles for this publication at: <https://www.researchgate.net/publication/230712024>

# Schiff Base Structured Acid–Base Cooperative Dual Sites in an Ionic Solid Catalyst Lead to Efficient Heterogeneous Knoevenagel Condensations

ARTICLE *in* CHEMISTRY - A EUROPEAN JOURNAL · OCTOBER 2012

Impact Factor: 5.73 · DOI: 10.1002/chem.201201338 · Source: PubMed

---

CITATIONS

14

---

READS

33

6 AUTHORS, INCLUDING:



Guojian Chen

Jiangsu Normal University

21 PUBLICATIONS 121 CITATIONS

SEE PROFILE



Jun Huang

South China University of Technology

79 PUBLICATIONS 2,826 CITATIONS

SEE PROFILE

# Schiff Base Structured Acid–Base Cooperative Dual Sites in an Ionic Solid Catalyst Lead to Efficient Heterogeneous Knoevenagel Condensations

Mingjue Zhang,<sup>[a]</sup> Pingping Zhao,<sup>[a]</sup> Yan Leng,<sup>[b]</sup> Guojian Chen,<sup>[a]</sup> Jun Wang,<sup>\*,[a]</sup> and Jun Huang<sup>[a]</sup>

**Abstract:** An acid–base bifunctional ionic solid catalyst [PySaIm]<sub>3</sub>PW was synthesized by the anion exchange of the ionic-liquid (IL) precursor 1-(2-salicylaldehyde)pyridinium bromide ([PySaIm]Br) with the Keggin-structured sodium phosphotungstate (Na<sub>3</sub>PW). The catalyst was characterized by FTIR, UV/Vis, XRD, SEM, Brunauer–Emmett–Teller (BET) theory, thermogravimetric analysis, <sup>1</sup>H NMR spectroscopy, ESI-MS, elemental analysis, and melting points. Together with various counterparts, [PySaIm]<sub>3</sub>PW was evaluated in Knoevenagel condensation under solvent and solvent-free conditions. The Schiff base structure attached to the IL cation of [PySaIm]<sub>3</sub>PW involves acidic salicyl hydroxyl and basic

imine, and provides a controlled nearby position for the acid–base dual sites. The high melting and insoluble properties of [PySaIm]<sub>3</sub>PW are relative to the large volume and high valence of PW anions, as well as the intermolecular hydrogen-bonding networks among inorganic anions and IL cations. The ionic solid catalyst [PySaIm]<sub>3</sub>PW leads to heterogeneous Knoevenagel condensations. In solvent-free condensation of benzaldehyde with ethyl cyanoacetate, it exhibits a conversion of

95.8% and a selectivity of 100%; the conversion is even much higher than that (78.2%) with ethanol as a solvent. The solid catalyst has a convenient recoverability with only a slight decrease in conversion following subsequent recyclings. Furthermore, the new catalyst is highly applicable to many substrates of aromatic aldehydes with activated methylene compounds. On the basis of the characterization and reaction results, a unique acid–base cooperative mechanism within a Schiff base structure is proposed and discussed, which thoroughly explains not only the highly efficient catalytic performance of [PySaIm]<sub>3</sub>PW, but also the lower activities of various control catalysts.

**Keywords:** heterogeneous catalysis • heteropolyacids • ionic liquids • Knoevenagel condensation • Schiff bases

## Introduction

Knoevenagel condensation of a carbonyl functionality with an activated methylene compound is a classic C–C bond-forming reaction for producing important intermediates in the fine-chemicals industry.<sup>[1,2]</sup> It is catalyzed by bases<sup>[3]</sup> or acids.<sup>[4]</sup> A number of researchers have revealed the effectiveness of acid–base bifunctional catalysts<sup>[5]</sup> on account of the synchronic activation of carbonyl on acid sites and the capture of the proton from methylene on basic sites.<sup>[6]</sup> On the other hand, ionic liquids (ILs) are well-known reaction

media with the advantages of low volatility, high thermal stability, adjustable solubility, and versatile structures.<sup>[7]</sup> In particular, “task-specific” IL catalysts tethered with basic and/or acidic functional groups have been reported for Knoevenagel reactions.<sup>[3c,d,4]</sup> For example, Boronat et al.<sup>[5g]</sup> prepared an acid–base IL catalyst, [diamine-A]BF<sub>4</sub>, with every acid and base site being separated by a –CH<sub>2</sub>– group. It showed improved activity for the condensation of benzaldehyde with methylene compounds. However, that system needed a large amount of IL (20 mol %), and the resultant homogeneous reaction encountered difficulty in catalyst recycling. To realize convenient catalyst recovery, efforts have been made to prepare heterogeneous bifunctional catalysts by supporting organic bases on acidic porous carriers;<sup>[5a,f]</sup> nevertheless, this approach could not control the distance between acid and base sites, which is a key influential factor for an acid–base bifunctional catalyst to enhance the reactivity of a Knoevenagel condensation.<sup>[8]</sup> Thus, it is of interest to design an efficient acid–base bifunctional catalyst with a controllable acid–base distance for heterogeneous Knoevenagel condensations.

Heteropolyacids (HPAs) have been widely used as the catalysts for organic transformations,<sup>[9]</sup> but the common Keggin HPAs with a strong intrinsic acidity are rarely used for Knoevenagel condensations. Significant advances in this

[a] M. Zhang, P. Zhao, G. Chen, Prof. Dr. J. Wang, Prof. Dr. J. Huang  
State Key Laboratory of Materials-Oriented  
Chemical Engineering  
College of Chemistry and Chemical Engineering  
Nanjing University of Technology  
Nanjing, Jiangsu, 210009 (P.R. China)  
Fax: (+86) 25-83172264  
E-mail: junwang@njut.edu.cn

[b] Dr. Y. Leng  
School of Chemical and Material Engineering  
Jiangnan University, Wuxi, Jiangsu  
214122 (P.R. China)

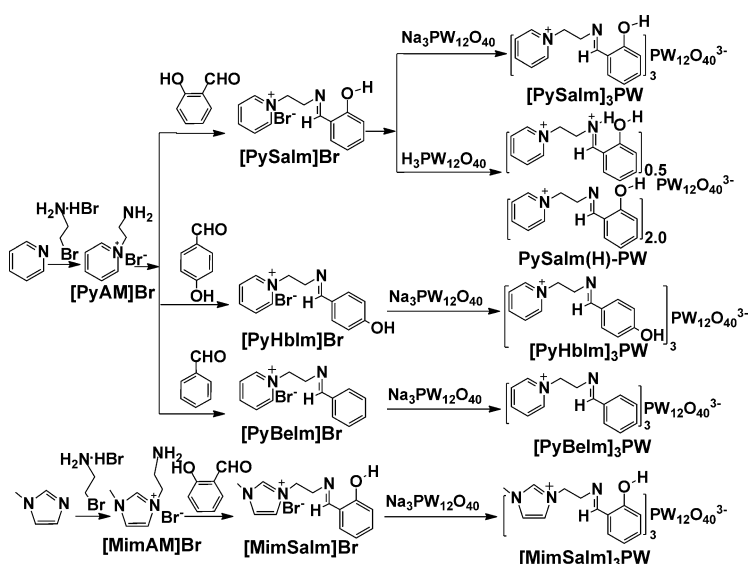
Supporting information for this article is available on the WWW under <http://dx.doi.org/10.1002/chem.201201338>.

area are the use of a unusual dimeric disilicoicosatungstate  $[\text{H}(\gamma\text{-SiW}_{10}\text{O}_{32})_2(\mu\text{-O})_4]^{7-}$  and its parent divacant  $\gamma$ -Keggin silicododecatungstate  $[\gamma\text{-SiW}_{10}\text{O}_{34}(\text{H}_2\text{O})_2]^{4-}$  as homogeneous basic catalysts,<sup>[10]</sup> and the development of a heterogeneous metal–organic framework (MOF) catalyst that encapsulates a  $\text{Cr}^{3+}$ -substituted lacunary HPA.<sup>[11]</sup> Another strategy for modifying HPA catalysts is the combination of HPA anions with organic cations through ionic linkages,<sup>[12]</sup> which is also an interesting topic in IL chemistry.<sup>[13]</sup> Recently, HPA–IL hybrids have been reported and applied in electrochemistry, phototropy, and materials science.<sup>[14]</sup> Furthermore, the structures of single crystals for some imidazolium salts with HPA anions have been determined.<sup>[15]</sup> In the field of catalysis, Luo et al.<sup>[16]</sup> modulated the stereoselectivity of homogeneous asymmetric C–C bond-forming reactions over a bifunctional catalyst that involved the basic sites of chiral amine ILs and the acidic centers of Keggin phosphotungstic acid. Our group<sup>[17]</sup> developed a series of HPA–IL ionic catalysts by pairing Keggin HPA anions with “task-specific” IL cations. Because of the high valence and large volume of HPA anions, the resulting catalysts were insoluble solid-state compounds, which mostly behaved as the heterogeneous catalysts for organic syntheses.

Moreover, as well-known ligands, Schiff bases have long attracted research interest for synthesis, structure, and reactivity in coordination chemistry, catalysis, and materials science.<sup>[18]</sup> In terms of ILs, Schiff bases have been attached to imidazolium tags for producing novel Schiff base ILs for recovering metal catalysts<sup>[19]</sup> or coordinating metal ions.<sup>[20]</sup> Actually, a Schiff base molecule itself involves a Lewis basic  $\text{C}=\text{N}$  and a weak Brønsted acidic  $\text{OH}$  group, with the acid–base distance being controlled by the Schiff base structure. Therefore, it should be very interesting to employ a Schiff base structure as an acid–base bifunctional catalytic unit for Knoevenagel condensations; however, to the best of our knowledge, there are no previous reports of Schiff base molecules being used in this way.

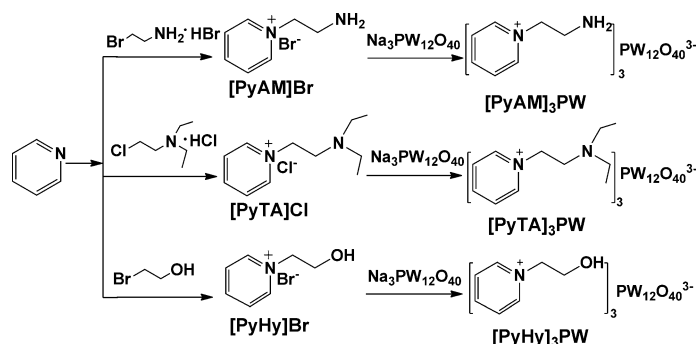
In this study, we prepared a HPA-based ionic solid  $[\text{PySaIm}]_3\text{PW}$  by pairing Keggin phosphotungstic HPA anions (PW) with pyridine-based Schiff base tethered IL cations ( $\text{PySaIm}$ ) (the top line of Scheme 1). This ionic catalyst is task-specifically designed for Knoevenagel reactions, because this Schiff base is not used as a traditional ligand for coordinating a metal, but as acid–base dual catalytic centers ( $\text{C}=\text{N}$ : base center;  $\text{OH}$ : acid center). To avoid protonation of the  $\text{C}=\text{N}$  groups in IL cations by a highly acidic HPA solution, neutral  $\text{Na}_3\text{PW}_{12}\text{O}_{40}$  was used as the ion exchanger instead of the customary  $\text{H}_3\text{PW}_{12}\text{O}_{40}$ . Characterizations and catalytic performances for Knoevenagel reactions were tested in detail over this HPA-based Schiff base tethered ionic catalyst.

To examine the rationality and effectiveness of the designing strategy for the target catalyst  $[\text{PySaIm}]_3\text{PW}$ , various counterpart hybrids were prepared for comparison (Scheme 1), including  $[\text{PyHbIm}]_3\text{PW}$  with the acid  $\text{OH}$  and base  $\text{C}=\text{N}$  sites separated by a phenyl ring;  $[\text{PyBeIm}]_3\text{PW}$ ,



Scheme 1. Synthesis of the HPA-based Schiff base tethered ionic catalyst  $[\text{PySaIm}]_3\text{PW}$  and various counterparts.

which bears only base  $\text{C}=\text{N}$ ;  $[\text{MimSaIm}]_3\text{PW}$  with pyridinium replaced by imidazolium; and  $\text{PySaIm}(\text{H})\text{-PW}$ , using the strong acidic  $\text{H}_3\text{PW}_{12}\text{O}_{40}$  as the ion exchanger. Other control samples  $[\text{PyAM}]_3\text{PW}$ ,  $[\text{PyTA}]_3\text{PW}$ , and  $[\text{PyHy}]_3\text{PW}$  were prepared by pairing PW anions with the respective commonly seen Schiff base free mono-basic or mono-acidic IL cations (Scheme 2).



Scheme 2. Synthesis of the control catalysts with Schiff base free mono-basic or mono-acidic IL cations.

## Results and Discussion

**Characterizations for  $[\text{PySaIm}]_3\text{PW}$ :**  $[\text{PySaIm}]_3\text{PW}$  was characterized by FTIR, UV/Vis, XRD, SEM, Brunauer–Emmett–Teller (BET) theory, thermogravimetric analysis (TGA),  $^1\text{H}$  NMR spectroscopy, ESI-MS, elemental analysis, and melting points (see the Experimental Section for details). The elemental analysis found (%) C 13.93, N 2.39, and H 1.24, which are close to calculated (%) values of C 14.11, N 2.35, and H 1.26, which provides the formula for  $[\text{PySaIm}]_3\text{PW}$  composed of three Schiff base tethered IL cations and one HPA anion. The TG curve (Figure S1 in the

Supporting Information) showed a stable structure for [PySaIm]<sub>3</sub>PW up to 230 °C. The slight weight loss at the early heating stage around 130 °C owes itself to the release of moisture and constitutional water, and the drastic weight loss above 230 °C is because of the decomposition of the organic moiety followed with the complete collapse of the inorganic Keggin HPA structure to form P<sub>2</sub>O<sub>5</sub> and WO<sub>3</sub>.<sup>[21]</sup> The total weight loss of 19.42 % in the range of 130–620 °C is close to the theoretical data of 19.75 %, which again verifies the chemical composition of [PySaIm]<sub>3</sub>PW shown in Scheme 1. Although it has an IL-like structure, [PySaIm]<sub>3</sub>PW has a high melting point of approximately 220 °C on account of the strong electrostatic interaction between the large-volume organic cation and the inorganic HPA anion with both large volume and high negative charge. [PySaIm]<sub>3</sub>PW is also insoluble in common standard solvents, including water, alcohols, acetone, acetonitrile, chlorinated hydrocarbons, THF, and DMF. These features make it possible for [PySaIm]<sub>3</sub>PW to be tried as a heterogeneous solid catalyst in liquid-phase organic transformations.

The SEM image in Figure 1 (Top) illustrates spherical particles for [PySaIm]<sub>3</sub>PW with sizes of approximately 0.05–0.2 μm. The observed submicrometer pores accumulated by the particles account for its BET specific surface area of 8.1 m<sup>2</sup> g<sup>−1</sup>. The XRD patterns of [PySaIm]<sub>3</sub>PW and pure Na<sub>3</sub>PW<sub>12</sub>O<sub>40</sub> are shown in Figure 1 (Bottom). Na<sub>3</sub>PW<sub>12</sub>O<sub>40</sub> presented a set of diffraction peaks for the typical crystal structure of sodium HPA salt finely arranged by the Keggin PW anions. For the organic HPA salt [PySaIm]<sub>3</sub>PW, however, those peaks disappeared, which indicates an amorphous phase. It is suggested that the substitution of Na<sup>+</sup> by the large PySaIm<sup>+</sup> IL cations has resulted in the loss of the long-range crystal order of PW anions. The only weak and broad Bragg reflection at approximately 8.6° implies micro-sized gaps among cations and anions,<sup>[22]</sup> which makes no contribution to the surface area tested by a nitrogen physiosorption.

Figure 2 displays the FTIR spectra of the selected samples. For [PySaIm]<sub>3</sub>PW, the bands at 1631 cm<sup>−1</sup> assigned to the stretching vibration of −C=N in imine, 3444 cm<sup>−1</sup> to −OH, and 1276 cm<sup>−1</sup> to C–O in an aromatic ring, are respectively similar to the observations at 1632, 3413, and 1277 cm<sup>−1</sup> for the IL precursor [PySaIm]Br.<sup>[23,24]</sup> Further, for the bending vibration of the C–H bond in pyridine, [PySaIm]<sub>3</sub>PW presented an almost identical band at 684 cm<sup>−1</sup> to that of [PySaIm]Br at 683 cm<sup>−1</sup>. These results demonstrate that [PySaIm]<sub>3</sub>PW has the same pyridinium-based Schiff base tethered IL cation as the precursor sample [PySaIm]Br. On the other hand, the four bands at 1094, 953, 858, and 808 cm<sup>−1</sup> featured for the Keggin structure of neat Na<sub>3</sub>PW<sub>12</sub>O<sub>40</sub> are attributed to P–O<sub>a</sub> (central oxygen), W=O (terminal oxygen), W–O<sub>b</sub>–W (corner-sharing oxygen), and W–O<sub>c</sub>–W (edge-sharing oxygen), respectively.<sup>[25]</sup> For [PySaIm]<sub>3</sub>PW, the four Keggin bands were detected clearly, thus indicating that the framework structure of the PW anion is thoroughly preserved. However, the shifts of the Keggin bands for [PySaIm]<sub>3</sub>PW indicate the distortion of

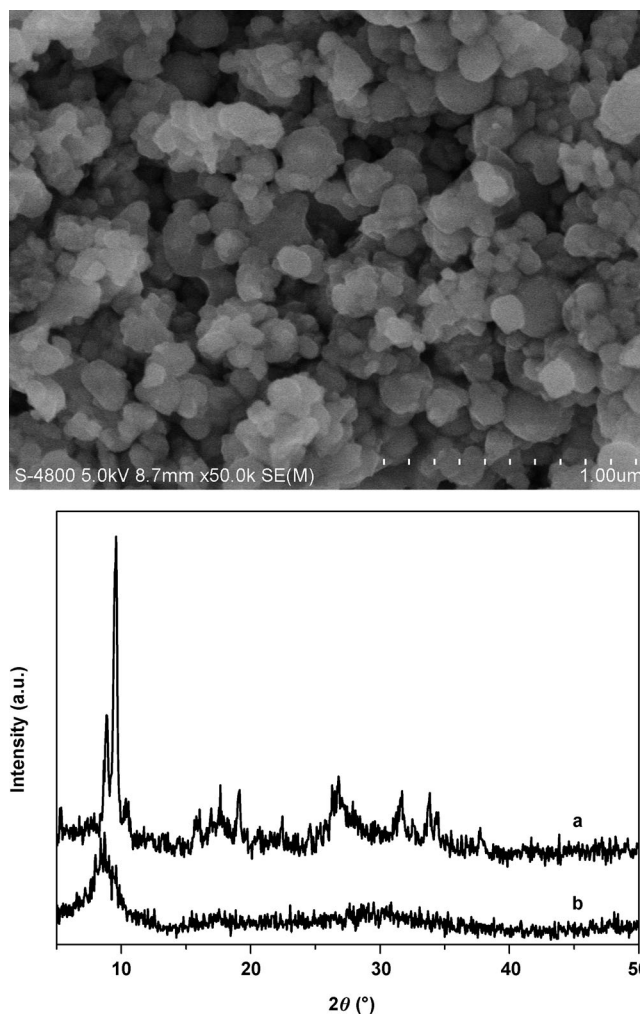


Figure 1. Top) SEM image of [PySaIm]<sub>3</sub>PW. Bottom) XRD patterns of a) Na<sub>3</sub>PW<sub>12</sub>O<sub>40</sub> and b) [PySaIm]<sub>3</sub>PW.

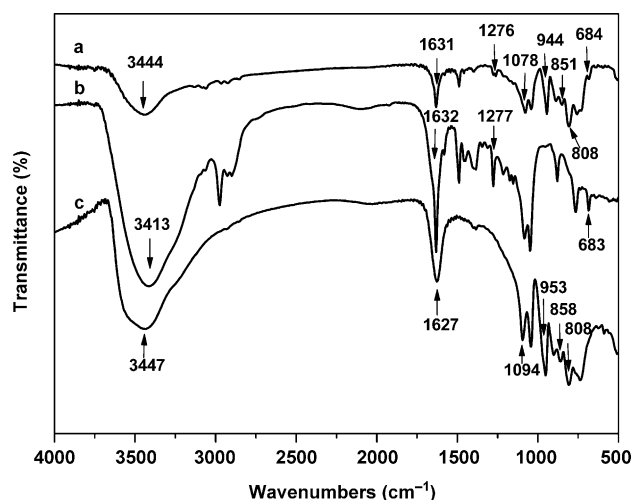
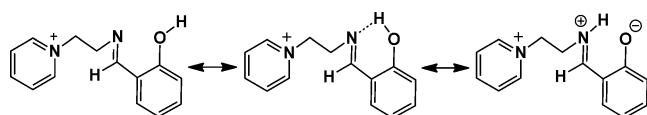


Figure 2. FTIR spectra of a) [PySaIm]<sub>3</sub>PW, b) [PySaIm]Br, and c) Na<sub>3</sub>PW<sub>12</sub>O<sub>40</sub>.

the Keggin framework on account of the extension of the conjugated  $\pi$  electrons from organic cations to inorganic anions.<sup>[26]</sup>

The previous result for the crystal structure of a pure Schiff base revealed a fundamental chemical phenomenon called keto–enol tautomerism between the –OH hydrogen and –C=N nitrogen atoms.<sup>[23]</sup> In Figure 2, the broad band around 3413  $\text{cm}^{-1}$  for [PyBeIm]Br also indicates the formation of the intermolecular hydrogen bonding within a Schiff base structure between the proton of –OH in salicyl and the nitrogen in imine, as proposed in Scheme 3. However, for



Scheme 3. Resonance structures for the proposed Schiff base of the phenolic form, intramolecular hydrogen bonding, and protonated imine in pyridine-based IL cation [PySaIm]<sup>+</sup>.

the HPA-paired analogue [PySaIm]<sub>3</sub>PW, the intensity of the corresponding band at 3444  $\text{cm}^{-1}$  was weakened drastically, which indicates that the presence of PW anions has greatly hindered the formation of the intramolecular hydrogen bonding. Alternatively, the extended intermolecular hydrogen-bonding networks are generated between IL cations and PW anions<sup>[27]</sup> in addition to the strong electrostatic interaction. This is a reason for the solid nature of [PySaIm]<sub>3</sub>PW.

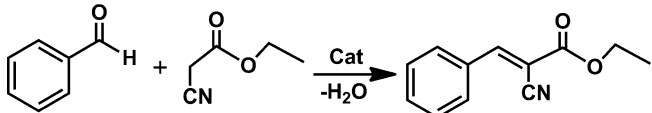
The intramolecular electronic behavior in the organic moiety of [PySaIm]<sub>3</sub>PW was further measured by the UV/Vis spectrum (Figure S2 in the Supporting Information). The adsorption bands in the range of 210–300 nm are attributed to the  $\pi$ – $\pi^*$ -electron transitions of benzene rings.<sup>[28]</sup> Though partly overlapped by the  $\pi$ – $\pi^*$  bands, the shoulder peak at 315 nm assigned to the free phenolic form near the imine group was observed clearly.<sup>[29]</sup> In addition, the broad and weak band at 415 nm reflects the ionic tautomer of the protonated imine (Scheme 3), which results from the intramolecular proton transfer from the salicyl –OH to the nitrogen atom of imine. The higher intensity of the peak of the 315 nm band over that of 415 nm, together with the lowered IR band at 3444  $\text{cm}^{-1}$  (Figure 2, curve a), allows one to infer that the phenolic form of the Schiff base structure predominates in the pyridine-based IL cation of [PySaIm]<sub>3</sub>PW. As a potential catalyst for Knoevenagel condensations, [PySaIm]<sub>3</sub>PW with such unaltered sal-

icyl –OH and imine groups in the Schiff base structure would play dual roles of acidic and basic catalytic centers.

### Knoevenagel condensation of benzaldehyde and ethyl cyanoacetate over various catalysts with ethanol as the solvent:

It is known that the polarity of a solvent can significantly affect the reaction rate of a Knoevenagel condensation, and a polar protic solvent such as ethanol might help to activate the carbonyl substrate.<sup>[30]</sup> Accordingly, we first carried out the condensation of benzaldehyde and ethyl cyanoacetate in the presence of ethanol solvent over various catalysts, with results listed in Table 1. [PySaIm]<sub>3</sub>PW exhibited a GC conversion of 93.8% and a selectivity for ethyl (*E*)- $\alpha$ -cyanocinnamate of 100%, with an isolated yield of 86.5% (Table 1, entry 1). On account of the insolubility of the ionic-solid catalyst in this polar reaction mixture, the condensation process was a liquid–solid heterogeneous catalysis system. In contrast, the IL [PySaIm]Br caused a homogeneous reaction and demonstrated a perfect 100% selectivity with a conver-

Table 1. Comparison of the catalytic performances of [PySaIm]<sub>3</sub>PW with various control samples for the Knoevenagel condensation of benzaldehyde and ethyl cyanoacetate with ethanol as the solvent.<sup>[a]</sup>



Entry	Catalyst	Solubility in reaction	Conversion <sup>[b]</sup> [%]	Selectivity <sup>[c]</sup> [%]
1	[PySaIm] <sub>3</sub> PW	insoluble	93.8	100 (86.5)
2	[PySaIm]Br	soluble	91.4	100
3	PySaIm(H)–PW	insoluble	32.0	(26.8)
4	[PyHbIm] <sub>3</sub> PW	insoluble	75.3	100
5	[MimSaIm] <sub>3</sub> PW	insoluble	81.4	100
6	[PyBeIm] <sub>3</sub> PW	insoluble	65.6	100
7	[PyTA] <sub>3</sub> PW	insoluble	67.8	100
8	[PyAM] <sub>3</sub> PW	insoluble	77.0	100
9	[PyHy] <sub>3</sub> PW	insoluble	60.3	100
10	without	–	25.7	100

[a] Reaction conditions: catalyst (0.1 g; 0.027 mmol for [PySaIm]<sub>3</sub>PW), benzaldehyde (8 mmol), ethyl cyanoacetate (8 mmol), ethanol (5 mL), 70 °C, 4 h. [b] GC conversion based on ethyl cyanoacetate. [c] GC selectivity (isolated yield in parenthesis) for the target product ethyl (*E*)- $\alpha$ -cyanocinnamate, m.p.: 49–50 °C; <sup>1</sup>H NMR (300 MHz, CDCl<sub>3</sub>):  $\delta$  = 1.40 (t, 3H), 4.39 (q, 2H), 7.48–7.59 (m, 3H), 8.00 (d, 2H), 8.25 ppm (s, 1H) (see Figure S3 in the Supporting Information).

sion of 91.4% (Table 1, entry 2). One can see that the heterogeneous catalyst [PySaIm]<sub>3</sub>PW is even more active than the homogeneous [PySaIm]Br, with the added advantage of much easier recovery from a reacted mixture.

Noticeably, relative to [PySaIm]<sub>3</sub>PW, all the PW-paired IL-like counterparts presented lower catalytic activities for the same condensation reaction (Table 1, entries 3–9). When using H<sub>3</sub>PW<sub>12</sub>O<sub>40</sub> instead of Na<sub>3</sub>PW<sub>12</sub>O<sub>40</sub> as the starting material to conduct the anion exchange with [PySaIm]Br, the obtained hybrid PySaIm(H)–PW gave a conversion of 32.0%, which is at a similarly low level to the noncatalyst system (Table 1, entries 3 and 10). The extremely low activity is associated with the partial elimination of the basicity of imine groups in the Schiff base structure on account of the protonation by the highly acidic H<sub>3</sub>PW<sub>12</sub>O<sub>40</sub>.<sup>[17c,d]</sup> Very inter-

estingly, [PyHbIm]<sub>3</sub>PW, although it has an analogous structure to [PySaIm]<sub>3</sub>PW, showed a remarkably lower conversion of 75.3% (Table 1, entry 4). This result arises from the much longer distance between acid and base sites separated by a benzene ring in the organic cation unit, which agrees with the earlier statement that the acid–base distance would greatly influence Knoevenagel reactions.<sup>[8]</sup> Furthermore, when the pyridine ring of [PySaIm]<sub>3</sub>PW was replaced by the more commonly used imidazole ring in IL cations, the resulting ionic solid [MimSaIm]<sub>3</sub>PW displayed a lower conversion of 81.4% (Table 1, entry 5). This seems to be relative to the stronger acidity of the C-2 protons in imidazolium compounds.<sup>[3c,31]</sup> [PyBeIm]<sub>3</sub>PW is also an analogue sample of [PySaIm]<sub>3</sub>PW, with the hydroxyl being removed from the benzene ring, thus its much lower conversion of 65.6% (Table 1, entry 6) owes itself to the loss of acidic sites. Other mono-base and mono-acid catalysts [PyAM]<sub>3</sub>PW, [PyTA]<sub>3</sub>PW, and [PyHy]<sub>3</sub>PW, which were prepared by using Schiff base free pyridine-based IL cations, also showed much lower activities (Table 1, entries 7–9).

The above comparisons demonstrate that the high activity of [PySaIm]<sub>3</sub>PW toward the heterogeneous Knoevenagel condensation is closely related to its unique structure: the high-valent PW anion endows the ionic catalyst with a solid nature for the heterogeneity of the reaction, and the Schiff base tethered pyridinium IL cation provides acid and base dual active sites with suitable strength and spacing distance.

**Solvent-free Knoevenagel condensation of benzaldehyde and ethyl cyanoacetate over various catalysts:** As has been indicated in Table 1, [PySaIm]<sub>3</sub>PW is a good heterogeneous catalyst for the Knoevenagel condensation in the presence of ethanol solvent. However, there is already a considerable amount of organic component in [PySaIm]<sub>3</sub>PW, and it is thus reasonable to consider that the hydroxyl-containing organic moiety therein might function as a polar protic solvent. Accordingly, we further attempted the solvent-free Knoevenagel condensation of benzaldehyde and ethyl cyanoacetate over [PySaIm]<sub>3</sub>PW, with results shown in Table 2. As expected, without a solvent, [PySaIm]<sub>3</sub>PW still behaved

like a heterogeneous catalyst and gave a very high conversion of 95.8% and selectivity of 100%, coupled with an isolated yield of 88.3% (Table 2, entry 1). The conversion is much higher than the result of 78.2% (Table 2, entry 2) under the ethanol solvent conditions with the same reaction time of 2 h. In fact, a considerably high conversion of 90.3% could be obtained without using any external solvents and within a short time of 45 min (Table 2, entry 3). Moreover, entry 4 of Table 2 even offered a perfect 100% conversion with 100% selectivity if the amount of the substrate ethyl cyanoacetate were reduced from 8 to 7 mmol under solvent-free conditions. Consequently, one can see that [PySaIm]<sub>3</sub>PW is an excellent heterogeneous catalyst under solvent-free conditions. On the other hand, very high conversion and selectivity could be observed over the parent IL catalyst [PySaIm]Br, but it is a homogeneous catalyst (Table 2, entry 5).

In contrast to [PySaIm]<sub>3</sub>PW, all the pyridine-based control samples exhibited much lower activities. For the hydroxyl-free catalysts [PyBeIm]<sub>3</sub>PW, [PyTA]<sub>3</sub>PW, and [PyAM]<sub>3</sub>PW (Table 2, entries 6–8), the absence of ethanol solvent caused sharp decreases in activities: their conversions were more or less as low as that of the uncatalyzed reaction (Table 2, entry 11). The mono-acid catalyst [PyHy]<sub>3</sub>PW, which bears hydroxyl groups in its organic moiety, showed a conversion of 35.6% (Table 2, entry 9); though far from a high value, it is obviously higher than those of the three hydroxyl-free counterparts. These results suggest a “solvent role” of the hydroxyl-containing organic moiety in the absence of an external solvent. However, the hydroxyl-containing acid–base bifunctional catalyst [PyHbIm]<sub>3</sub>PW (Table 2, entry 10) exhibited a lower conversion of 50.3% than [PySaIm]<sub>3</sub>PW, mostly due to the longer distance from the acid to base sites separated by a benzene ring.

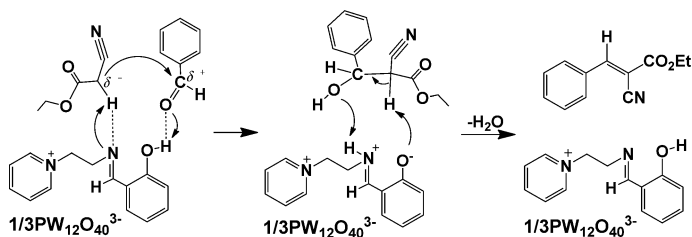
**Proposed acid–base cooperative mechanism for the [PySaIm]<sub>3</sub>PW-catalyzed Knoevenagel reaction:** On the basis of the above characterizations and reaction measurements, as well as the previous results for the acid–base bifunctional IL<sup>[5g]</sup> and supported catalysts,<sup>[5f]</sup> an acid–base cooperative mechanism for the [PySaIm]<sub>3</sub>PW-catalyzed Knoevenagel condensation is proposed in Scheme 4. The new reaction route is very different from the early imine-intermediated or ion-pair processes.<sup>[32]</sup> In Scheme 4, the weakly acidic proton of –OH in salicyl interacts with the oxygen of a carbonyl group in benzaldehyde, through which the C=O bond is polarized with the increase in the positive charge on the carbon of the carbonyl group. Meanwhile, as a Lewis basic site, the lone-electron-pair-bear-

Table 2. Solvent-free Knoevenagel condensation of benzaldehyde with ethyl cyanoacetate over various catalysts.<sup>[a]</sup>

Entry	Catalyst	Solubility in reaction	Conversion <sup>[b]</sup> [%]	Selectivity <sup>[c]</sup> [%]
1	[PySaIm] <sub>3</sub> PW	insoluble	95.8	100 (88.3)
2 <sup>[d]</sup>	[PySaIm] <sub>3</sub> PW	insoluble	78.2	100
3 <sup>[e]</sup>	[PySaIm] <sub>3</sub> PW	insoluble	90.3	100
4 <sup>[f]</sup>	[PySaIm] <sub>3</sub> PW	insoluble	100	100
5	[PySaIm]Br	soluble	94.4	100
6	[PyBeIm] <sub>3</sub> PW	insoluble	12.5	100
7	[PyTA] <sub>3</sub> PW	insoluble	23.9	100
8	[PyAM] <sub>3</sub> PW	insoluble	18.2	100
9	[PyHy] <sub>3</sub> PW	insoluble	35.6	100
10	[PyHbIm] <sub>3</sub> PW	insoluble	50.3	100
11	without	–	13.7	100

[a] Reaction conditions: catalyst (0.1 g; 0.027 mmol for [PySaIm]<sub>3</sub>PW), benzaldehyde (8 mmol), ethyl cyanoacetate (8 mmol), 70 °C, 2 h. [b] GC conversion based on ethyl cyanoacetate. [c] Selectivity (isolated yield in parentheses) for ethyl (*E*)- $\alpha$ -cyanocinnamate. [d] Ethanol as solvent, 2 h, other conditions (see Table 1). [e] Reaction time: 45 min. [f] Using 7 mmol ethyl cyanoacetate.





Scheme 4. The acid–base cooperative mechanism proposed for the heterogeneous Knoevenagel condensation catalyzed by the Schiff base tethered [PySaIm]<sub>3</sub>PW ionic hybrid.

ing nitrogen of an imine group attacks the electron-deficient methylene hydrogen, thus forming a methylene carbanion. These catalytic activation processes take place within the tethered Schiff base structure of [PySaIm]<sub>3</sub>PW. It is the Schiff base structure that provides a proximate position for the acid and base sites with a suitably short distance, thereby allowing a prompt further reaction of the methylene carbanion with the positive-charged carbon of carbonyl into the C–C-bonded intermediate that links the two reactants. Finally, the product ethyl cyanocinnamate is obtained by an immediate elimination of a water molecule from the intermediate, from which the ionic catalyst [PySaIm]<sub>3</sub>PW is released for the next catalysis cycle.

The catalytic roles of the basic nitrogen sites in amino or imino functional groups for Knoevenagel condensations have been revealed by previous reports,<sup>[3,5,6]</sup> which supports the idea of the catalytic function of the basic imine in the Schiff base unit of [PySaIm]<sub>3</sub>PW for activating the methylene substrate in Scheme 4. In addition, the participation of the salicyl –OH as a catalytic acid site in the condensation reaction is evidenced by the FTIR spectra in Figure 3. Relative to the fresh [PySaIm]<sub>3</sub>PW (Scheme 4, curve a), the benzaldehyde-treated catalyst (Scheme 4, curve b) showed a band at 1688 cm<sup>−1</sup> that is assigned to the physically adsorbed benzaldehyde. More importantly, a small new band at

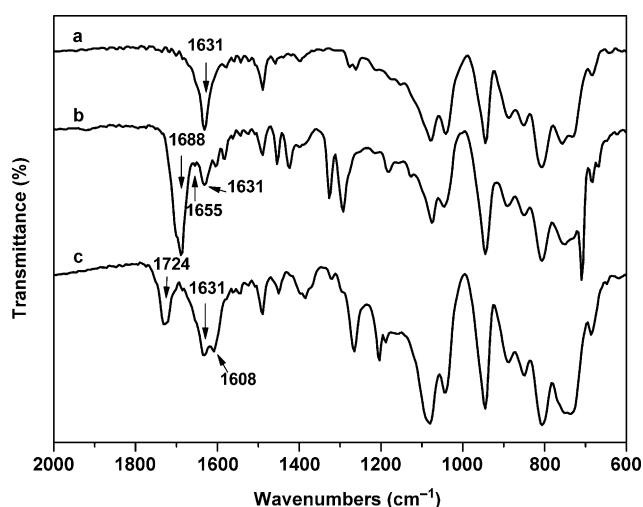
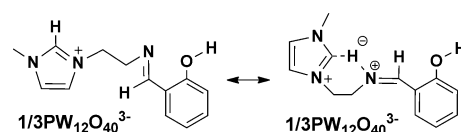


Figure 3. FTIR spectra of a) fresh [PySaIm]<sub>3</sub>PW, b) benzaldehyde-treated [PySaIm]<sub>3</sub>PW, and c) recovered [PySaIm]<sub>3</sub>PW.

1655 cm<sup>−1</sup> was detected, which strongly indicates the occurrence of polarized C=O groups that arise from the activation of carbonyls by the acidic proton of salicyl –OH.<sup>[5a]</sup> However, the recovered [PySaIm]<sub>3</sub>PW catalyst from a reacted mixture (Scheme 4, curve c) did not show that polarized C=O band, thereby confirming the catalytic role of the salicyl hydroxyl as a weak acid. It is known that the effect of a commonly used polar protic solvent such as ethanol for a Knoevenagel reaction is the aided activation of the carbonyl substrate.<sup>[30]</sup> Now that the hydroxyl in the Schiff base structure of the organic moiety of [PySaIm]<sub>3</sub>PW has acted as the catalytic acid center for activating the carbonyl substrate, as indicated in Scheme 4, the excellent catalytic performance of [PySaIm]<sub>3</sub>PW in the absence of an external polar solvent is understandable (Table 2).

The acid–base cooperative mechanism within a Schiff base structure in Scheme 4 satisfactorily accounts for the decreased activities of various control catalysts relative to [PySaIm]<sub>3</sub>PW (Tables 1 and 2). The protonated imine in PySaIm(H)–PW greatly eliminates the basicity of the Schiff base, and thus hinders the acid–base cooperative function, thereby resulting in drastically lower conversion. For [PyHbIm]<sub>3</sub>PW, the weak hydroxyl acid and the imine base are concurrent in one molecule, which seems similar to [PySaIm]<sub>3</sub>PW, but the longer distance from acid to base separated by a benzene ring would slow the reaction rate for generating the C–C-bonded intermediate. On the other hand, the fact that both the mono-base (e.g., [PyBeIm]<sub>3</sub>PW, [PyAM]<sub>3</sub>PW, or [PyTA]<sub>3</sub>PW) and the mono-acid (e.g., [PyHy]<sub>3</sub>PW) catalysts showed sharp decreases in activity strongly implies the highly efficient performance of the acid–base cooperative mechanism for [PySaIm]<sub>3</sub>PW.

It is also interesting to see that the imidazolium-substituted control sample [MimSaIm]<sub>3</sub>PW, which contains exactly the same Schiff base structure as the pyridinium-based [PySaIm]<sub>3</sub>PW, presented a much lower activity (Table 1). Taking into account of the stronger acidity of C-2 protons in imidazolium,<sup>[3c,31]</sup> a resonance structure that originated from the intramolecular protonation of the organic moiety of [MimSaIm]<sub>3</sub>PW is proposed in Scheme 5. The protonation



Scheme 5. Proposed resonance structures for the imidazolium-based IL cation of [MimSaIm]<sub>3</sub>PW.

of the basic imine by the C-2 proton of an imidazolium might suppress the full extent of the acid–base cooperative procedure within the Schiff base structure, which is responsible for the low activity of [MimSaIm]<sub>3</sub>PW.

According to Scheme 4, one might consider that the IL precursor [PySaIm]Br should display the highest activity because it has an identical pyridine-based Schiff base tethered organic cation to that of [PySaIm]<sub>3</sub>PW, together with the

most mass-transfer-favored homogeneous nature for the reaction. Nevertheless, [PySaIm]Br was slightly less active than the heterogeneous catalyst [PySaIm]<sub>3</sub>PW (Tables 1 and 2). The stronger intramolecular interaction between the hydroxyl of salicyl and the nitrogen of imine has been revealed in the Schiff base structure of the IL cation of [PySaIm]Br. Consequently, the formation of a significant amount of intramolecular hydrogen bonding and/or protonated imine (Figure 2 and Scheme 3) lowers the efficiency of the acid–base cooperative mechanism. Another reason is ascribed to the widely accepted concept of “pseudoliquid behavior” for a HPA catalyst,<sup>[33]</sup> that is, the ionic compound [PySaIm]<sub>3</sub>PW behaves as a bulk-type catalyst that allows polar substrates to penetrate its amorphous secondary structure, in which the substrates seem to be dissolved in the organic moiety for starting the acid–base cooperative catalysis. As a result, the bulk-type catalysis of [PySaIm]<sub>3</sub>PW does not relate to the low specific BET surface area of 8.1 m<sup>2</sup> g<sup>−1</sup>.

Based on the conversion of 90.3% in entry 3 of Table 2, [PySaIm]<sub>3</sub>PW gives a turnover number (TON) of 118.9 mol base site<sup>−1</sup> h<sup>−1</sup> in the condensation of benzaldehyde with ethyl cyanoacetate. Thus, the present bulk-type heterogeneous catalyst is much more active than the previously reported surface-type acid–base bifunctional catalyst, dihydroimidazole-functionalized, mesoporous molecular sieve SBA-15 (TON: 18.7 mol base site<sup>−1</sup> h<sup>−1</sup>), even with a very high BET surface area of 610 m<sup>2</sup> g<sup>−1</sup>.<sup>[5f]</sup> The main reason for the lower activity of this supported acid–base bifunctional catalyst is the impossibility to control the distance between the loaded organic basic sites and the acid sites on the surface of the silica support.

Therefore, the high efficiency of the acid–base cooperative mechanism for the [PySaIm]<sub>3</sub>PW-catalyzed Knoevenagel reaction thoroughly reflects the rational design strategy for the present catalyst, [PySaIm]<sub>3</sub>PW.

**Reusability of [PySaIm]<sub>3</sub>PW catalyst for Knoevenagel condensation of benzaldehyde and ethyl cyanoacetate:** Since [PySaIm]<sub>3</sub>PW-catalyzed Knoevenagel condensation is a liquid–solid biphasic heterogeneous reaction, the catalyst [PySaIm]<sub>3</sub>PW could be recovered from a reacted mixture by filtration, washing, and vacuum drying. Figure 4 plots two parallels of five-run catalyst recycling results for solvent-free Knoevenagel condensation of benzaldehyde with ethyl cyanoacetate. By using only recovered catalyst without adding any fresh one at intervals of two runs (Figure 4, curve a), a perfect selectivity of 100% could always be obtained (not shown); but the conversion decreased gradually. The reused catalyst in the second run showed a conversion of 80.4%, which is clearly lower than the fresh one (95.8%). After the second run, the rate of decrease of the conversions slowed, and by the fifth run the recycled catalyst yielded a conversion of 74.8%. The decrease in conversion is associated with the catalyst recovery yield of 86.7% for the second run and 83.2% for the fifth run, which are calculated on the basis of the fresh catalyst amount of 0.1 g for the first run. The catalyst reduction quantity includes the inevitable loss during

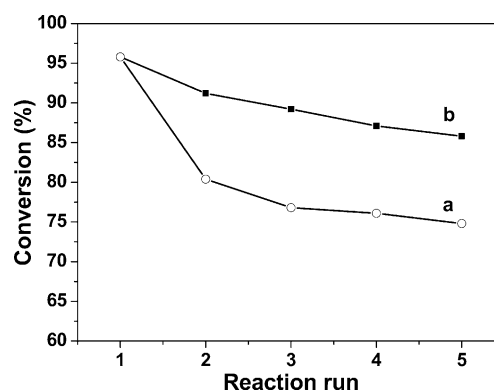


Figure 4. Catalytic reusability of [PySaIm]<sub>3</sub>PW for the Knoevenagel condensation of benzaldehyde and ethyl cyanoacetate: a) without adding fresh catalyst, b) with the addition of fresh catalyst to make the constant catalyst amount of 0.1 g.

the catalyst recovery operation and the leaching into the reaction solution. The similar decrease in activities for reused catalysts was also observed in previous reports on other HPA-IL ionic catalysts for esterifications.<sup>[17a,b]</sup>

To ascertain whether the loss of catalyst is the only reason for the reduced activities over recovered catalysts, another five run set of tests was investigated by using a constant catalyst amount of 0.1 g by mixing a small amount of fresh catalyst into the recovered one at recycling intervals (Figure 4, curve b). It showed higher conversions than that of Figure 4, curve a. However, the conversion still decreased, albeit very slowly. This result indicates that the reduced conversion is due not only to the loss of catalyst, but also the partial deactivation nature of the recovered catalyst itself. The FTIR spectrum for the recovered catalyst (Figure 3, curve c) illustrates generally similar bands to those of the fresh one, thereby implying the structural durability of the catalyst in this reaction. However, the extra bands detected at 1724 and 1608 cm<sup>−1</sup> are assigned to the C=O bond of ethyl cyanoacetate and the C=C of ethyl cyanocinnamate, respectively, which indicates that the recovered ionic solid involves residues from the reaction mixture that must have partially contaminated the acid/base sites, thereby resulting in a slight deactivation of the recovered catalyst. Additionally, the detection of the irremovable functional groups of substrate molecules in the recovered catalyst might be evidence of the supposed bulk-type catalysis due to the “pseudoliquid behavior” of [PySaIm]<sub>3</sub>PW.

**Solvent-free Knoevenagel condensations with various substrates over the [PySaIm]<sub>3</sub>PW catalyst:** To examine the scope of the [PySaIm]<sub>3</sub>PW catalyst for Knoevenagel condensations, we tested the reactivity of various substrates of carbonyl or methylene compounds under solvent-free conditions. The results are summarized in Table 3. When reacting with ethyl cyanoacetate, the aldehyde derivative of furaldehyde showed a higher conversion of 97.0% at a much shorter time of 0.2 h than benzaldehyde did (95.8%, 2 h) (Table 3, entries 1 and 2). Similarly, the strong electron-with-



Table 3. Solvent-free Knoevenagel condensations with various substrates catalyzed by [PySaIm]<sub>3</sub>PW.<sup>[a]</sup>

$$\begin{array}{c} \text{R}^1 \\ \diagup \\ \text{C}=\text{O} \\ \diagdown \\ \text{R}^2 \end{array} + \begin{array}{c} \text{X} \\ \diagup \\ \text{C} \\ \diagdown \\ \text{Y} \end{array} \xrightarrow[\text{-H}_2\text{O}]{[\text{PySaIm}]_3\text{PW}} \begin{array}{c} \text{R}^1 \\ \diagup \\ \text{C}=\text{C} \\ \diagdown \\ \text{R}^2 \end{array} \begin{array}{c} \text{X} \\ \diagup \\ \text{C} \\ \diagdown \\ \text{Y} \end{array}$$

Entry	R <sup>1</sup>	R <sup>2</sup>	Substrate	X	Y	t [h]	Conversion <sup>[b]</sup> [%]	Selectivity <sup>[c]</sup> [%]
1	Ph	H		CN	CO <sub>2</sub> Et	2	95.8	100
2	2-fural	H		CN	CO <sub>2</sub> Et	0.2	97.0	100
3 <sup>[d]</sup>	4-NO <sub>2</sub> -Ph	H		CN	CO <sub>2</sub> Et	0.5	93.4	100
4	2-Cl-Ph	H		CN	CO <sub>2</sub> Et	0.4	95.6	100
5 <sup>[d]</sup>	4-OH-Ph	H		CN	CO <sub>2</sub> Et	6	92.7	100
6	nC <sub>3</sub> H <sub>7</sub>	H		CN	CO <sub>2</sub> Et	6	77.6	100
7	nC <sub>7</sub> H <sub>15</sub>	H		CN	CO <sub>2</sub> Et	8	68.4	100
8	-cC <sub>5</sub> H <sub>10</sub> -			CN	CO <sub>2</sub> Et	12	62.3	100
9	CH <sub>3</sub>	CH <sub>3</sub>		CN	CO <sub>2</sub> Et	12	61.7	100
10	Ph	H		CN		0.1	100	100
11	Ph	H		COCH <sub>3</sub>	CO <sub>2</sub> Et	20	67.4	100
12	Ph	H		CO <sub>2</sub> Et	CO <sub>2</sub> Et	20	44.8	100

[a] Reaction conditions: catalyst 0.1 g (0.027 mmol), aldehyde or ketone (8 mmol), methylene compound (8 mmol), 70 °C. [b] Entries 1–9: GC conversion based on ethyl cyanoacetate; entries 10–12: GC conversion based on benzaldehyde. [c] Selectivity for the respective main products. [d] With ethanol as the solvent (5 mL) for dissolving the solid substrates of aldehydes.

drawing groups (–NO<sub>2</sub> and –Cl) attached to aromatic aldehydes were also very reactive substrates (Table 3, entries 3 and 4). In contrast, the electron-donating hydroxyl-tethered aromatic aldehyde (Table 3, entry 5) required a much longer time to reach a high conversion. On the other hand, the aliphatic aldehydes (Table 3, entries 6 and 7) and ketones (Table 3, entries 8 and 9) exhibited lower conversions of 62–78% at long reaction times of around 6–12 h.

With benzaldehyde as the constant carbonyl substrate, entry 10 of Table 3 shows that the highly activated methylene compound malononitrile offered an excellent and complete conversion of 100% to the target alkene product within a short time of 0.1 h. Nevertheless, when ethyl acetoacetate (Table 3, entry 11) and diethyl malonate (Table 3, entry 12) were used as the methylene substrates, only low conversions were obtained, even after a very long time of 20 h.

Consequently, the heterogeneous catalyst [PySaIm]<sub>3</sub>PW is widely applicable to Knoevenagel condensations of aromatic aldehydes with the methylene compounds activated by electron-withdrawing functional groups. It is suggested that comparatively inert substrates such as aliphatic aldehydes, ketones, diethyl malonate, and so on demand stronger acid–base cooperative catalysts, which requires further study.

## Conclusion

We have developed a new acid–base bifunctional catalyst, [PySaIm]<sub>3</sub>PW, for Knoevenagel condensations. The synthesis strategy for this ionic solid catalyst requires pairing pyridine-based Schiff base tethered IL cations with Keggin-structured HPA anions. The novelty of this synthetic strategy for [PySaIm]<sub>3</sub>PW is the involvement of the catalytically active sites of both acid (the proton of salicyl hydroxyl) and base (the nitrogen of imine) within a Schiff base structure, which adds the advantage of a controllable acid–base dis-

tance. Also, the large volume and high valence of HPA anions result in the solid-state nature and insoluble properties of the ionic compound [PySaIm]<sub>3</sub>PW. In solvent-free condensation of benzaldehyde with ethyl cyanoacetate, [PySaIm]<sub>3</sub>PW exhibits heterogeneity, high conversion (95.8%), and perfect selectivity (100%), with the yield even being much higher than in the presence of the solvent ethanol. The solid catalyst [PySaIm]<sub>3</sub>PW can be conveniently recovered after a reaction, and a five-run recycling test shows only slight decreases in conversion for reused catalysts. Furthermore, the new catalyst is widely applicable to many substrates of aromatic aldehydes with activated methylene compounds. A unique acid–base cooperative mechanism within the Schiff base structure is proposed to account for the good catalytic performance of [PySaIm]<sub>3</sub>PW, as well as to explain the lower activities of various control catalysts. The catalysis strategy of this study might be a significant step towards the design of heterogeneous ionic-solid catalysts for more traditional liquid-phase organic syntheses.

## Experimental Section

**Materials and methods:** All chemicals were of analytical grade and used as received. FTIR spectra for catalyst samples in KBr discs were recorded using a Nicolet 360 FTIR instrument in the 4000–400 cm<sup>–1</sup> region. The solid UV/Vis spectrum was measured using a PE Lambda 950 spectrometer with BaSO<sub>4</sub> as an internal standard. XRD patterns were collected using a Bruker D8 Advance powder X-ray diffractometer with a Ni-filtered Cu<sub>Kα</sub> radiation source at 40 kV and 20 mA, from 5 to 50° at a scan rate of 2 °C min<sup>–1</sup>. Before measurements, the samples were dried at 100 °C for 2 h. SEM images were recorded using a Hitachi S-4800 field-emission scanning electron microscope. BET surface areas were measured at the temperature of liquid nitrogen using a Micromeritics ASAP2010 analyzer. The samples were degassed at 150 °C to a vacuum of 10<sup>–3</sup> Torr before analysis. TG analysis was carried out using an STA409 instrument in dry air at a heating rate of 10 °C min<sup>–1</sup>. <sup>1</sup>H NMR spectra were measured using a Bruker DPX 300 spectrometer at ambient temperature in CDCl<sub>3</sub> or [D<sub>6</sub>]DMSO using TMS as the internal reference. The CHN elemental analysis was obtained using an elemental ana-

lyzer (FlashEA 1112). Melting points were determined using an X4 digital microscopic melting-point apparatus with an upper limit of 250 °C. Electrospray ionization mass spectrometry (ESI-MS) was recorded using a Finnigan Mat APISSQ 710 mass spectrometer.

**Synthesis of 1-(2-salicylaldehyde)pyridinium phosphotungstate [PySaIm]<sub>3</sub>PW (Scheme 1):** 1-(2-Aminoethyl)pyridinium bromide ([PyAM]Br) was synthesized according to the literature.<sup>[34]</sup> Pyridine (7.91 g, 100 mmol) and 2-bromoethylamine hydrobromide (20.49 g, 100 mmol) were dissolved in ethanol (50 mL) with stirring at 75 °C for 24 h under a nitrogen atmosphere. Upon completion, the solvent was removed by filtration, and the residue was washed twice with ethanol to afford [PyAM]Br·HBr as a white solid. KOH was added to the aqueous solution of the above solid for neutralization, followed by the evaporation under vacuum. Ethanol (25 mL) was then added into the resulting mixture with the appearance of the precipitated salt. After filtration, the filtrate was evaporated to give the product [PyAM]Br as dark brown oil (yield: 85 %). Afterwards, a mixture of [PyAM]Br (2.03 g, 10 mmol) and salicylaldehyde (1.22 g, 10 mmol) was stirred at room temperature for 12 h without a solvent, followed by washing with diethyl ether (3 × 30 mL) and vacuum evaporation,<sup>[20]</sup> which gave the IL product [PySaIm]Br (1-(2-salicylaldehyde)pyridinium bromide) as dark burgundy oil (yield: 79 %). <sup>1</sup>H NMR (300 MHz, [D<sub>6</sub>]DMSO, TMS): δ = 4.21 (t, 2H), 5.06 (t, 2H), 6.88 (q, 2H), 7.34 (m, 1H), 7.41 (d, 1H), 8.21 (t, 2H), 8.55 (s, 1H), 8.65 (t, 1H), 9.20 (d, 2H), 12.4 ppm (s, 1H) (see Figure S4 in the Supporting Information). Finally, [PySaIm]Br (1.84 g, 6.0 mmol) was added to the aqueous solution of Na<sub>3</sub>PW<sub>12</sub>O<sub>40</sub> in ethanol (5.76 g, 2.0 mmol) with further stirring at room temperature for 24 h. Bright yellow precipitate formed. It was filtered and washed with water three times, followed by drying in a vacuum to give the final product [PySaIm]<sub>3</sub>PW as a solid (yield: 95 %). MS (ESI)<sup>+</sup>: *m/z*: 227.1 [PySaIm]<sup>+</sup> (Figure S5A in the Supporting Information). Negative-ion ESI-MS showed a fragmentation pattern identical to that of PW<sub>12</sub>O<sub>40</sub><sup>3−</sup> (Figure S5B in the Supporting Information),<sup>[35a]</sup> with the following assignments for the clusters: *m/z*: 122.1 (H<sub>4</sub>PW<sub>2</sub>O<sub>13</sub>/5), 198.8 (H<sub>3</sub>W<sub>4</sub>O<sub>16</sub>/5), 226.4 (H<sub>4</sub>P<sub>2</sub>W<sub>3</sub>O<sub>18</sub>/4), 254.1 (PW<sub>5</sub>O<sub>20</sub>/5), 446.7 (H<sub>4</sub>PW<sub>9</sub>O<sub>34</sub>/5), 485.8 (PW<sub>10</sub>O<sub>35</sub>/5), 578.6 (H<sub>2</sub>PW<sub>7</sub>O<sub>26</sub>/3), 655.8 (H<sub>2</sub>PW<sub>8</sub>O<sub>29</sub>/3). Meanwhile, the patterns identical to those of possible cation/anion aggregates were observed (Figure S5B in the Supporting Information)<sup>[35b]</sup> with the following assignments: *m/z*: 684.4 [(C<sub>14</sub>H<sub>15</sub>N<sub>2</sub>O)<sub>4</sub>P<sub>2</sub>W<sub>7</sub>O<sub>30</sub>/4], 705.6 [(C<sub>14</sub>H<sub>15</sub>N<sub>2</sub>O)<sub>3</sub>W<sub>12</sub>O<sub>40</sub>/5], 781.7 [(C<sub>14</sub>H<sub>15</sub>N<sub>2</sub>O)<sub>3</sub>PW<sub>10</sub>O<sub>36</sub>/4].

**Synthesis of various control catalysts:** [PyHbIm]<sub>3</sub>PW and [PyBeIm]<sub>3</sub>PW were prepared according to Scheme 1, with the same method as described above for [PySaIm]<sub>3</sub>PW, except for the use of 4-hydroxybenzaldehyde and benzaldehyde as the respective starting raw materials instead of salicylaldehyde. PySaIm(H)–PW was prepared by using H<sub>3</sub>PW<sub>12</sub>O<sub>40</sub> to make the anion exchange instead of Na<sub>3</sub>PW<sub>12</sub>O<sub>40</sub>. The chemical composition of PySaIm(H)–PW is shown in Scheme 1, which was determined by elemental analysis (found (%): C 11.77, N 2.14, H 1.13). [MimSaIm]<sub>3</sub>PW was obtained according to the bottom line of Scheme 1, with imidazole replacing pyridine to prepare the Schiff based tethered IL cation. [PyAM]<sub>3</sub>PW, [PyTA]<sub>3</sub>PW, and [PyHy]<sub>3</sub>PW were prepared according to Scheme 2. For [PyAM]<sub>3</sub>PW, [PyAM]Br (1.22 g, 6.0 mmol) was added to the aqueous solution of Na<sub>3</sub>PW<sub>12</sub>O<sub>40</sub> in ethanol (5.76 g, 2.0 mmol), and then the mixture was stirred at room temperature for 24 h. Next, the formed dark yellow precipitate was filtered and washed with water three times, followed by drying in a vacuum to give the solid product [PyAM]<sub>3</sub>PW (yield: 94 %). [PyTA]<sub>3</sub>PW and [PyHy]<sub>3</sub>PW were prepared by following the same procedure, but with 2-piperidinoethyl chloride hydrochloride and ethylene bromohydrin as the starting materials, respectively.

**Procedures for Knoevenagel condensations:** A typical procedure for Knoevenagel condensation of benzaldehyde with ethyl cyanoacetate is as follows. Ethanol (solvent, 5 mL), benzaldehyde (0.849 g, 8 mmol), and ethyl cyanoacetate (0.905 g, 8 mmol) were added to a round-bottomed flask reactor (25 mL) equipped with a condenser under a nitrogen atmosphere. After the heating temperature was adjusted to 70 °C, the catalyst [PySaIm]<sub>3</sub>PW (0.1 g, 0.027 mmol) was added into the reactor, and then the reaction slurry was stirred for 4 h under reflux conditions. Following

the procedure, the solvent-free condensation reaction was also carried out at a shorter reaction time of 2 h without adding the ethanol solvent. After reaction, the reaction mixture was centrifuged to remove the solid catalyst, and the liquid was analyzed using a gas chromatograph (GC SP-6890) equipped with an FID detector and a capillary column (SE-54; 30 m × 0.32 mm × 0.25 μm). *n*-Dodecane was used as the internal standard to calculate the reaction conversion. Isolated yield was obtained by using column chromatography. A five-run catalyst recycling was carried out for testing the reusability of the catalyst. The catalyst was recovered from a reacted mixture by filtration, washing with diethyl ether three times, and vacuum drying. Another five-run catalyst recycling was carried out by adding a small amount of fresh catalyst to the recovered catalyst to make a constant total catalyst amount of 0.1 g. Also, the reactivity of various substrates of carbonyl or methylene compounds for Knoevenagel condensations was tested over the catalyst [PySaIm]<sub>3</sub>PW. In addition to [PySaIm]<sub>3</sub>PW, catalytic behaviors of the prepared control catalysts were measured under the typical reaction conditions for comparison.

## Acknowledgements

The authors thank greatly the Key Program of the National Natural Science Foundation of China (no. 21136005).

- [1] E. Knoevenagel, *Ber. Dtsch. Chem. Ges.* **1898**, *31*, 738–748.
- [2] a) A. Corma, R. M. Martín-Aranda, *Appl. Catal. A* **1993**, *105*, 271–279; b) A. Corma, R. M. Martín-Aranda, F. Sanchez, *Stud. Surf. Sci. Catal.* **1991**, *59*, 503–511.
- [3] a) C. H. Xing, S. Z. Zhu, *J. Org. Chem.* **2004**, *69*, 6486–6488; b) J. Gascon, U. Aktay, M. D. Hernandez-Alonso, G. P. M. van Klink, F. Kapteijn, *J. Catal.* **2009**, *261*, 75–87; c) S. A. Forsyth, U. Frohlich, P. Goodrich, H. Q. N. Gunaratne, C. Hardacre, A. McKeown, K. R. Seddon, *New J. Chem.* **2010**, *34*, 723–731; d) Y. Zhang, C. Xia, *Appl. Catal. A* **2009**, *366*, 141–147; e) N. Kan-nari, S. Okamura, S. Fujita, J. Ozaki, M. Araib, *Adv. Synth. Catal.* **2010**, *352*, 1476–1484.
- [4] J. R. Harjani, S. J. Nara, M. M. Salunkhe, *Tetrahedron Lett.* **2002**, *43*, 1127–1130.
- [5] a) A. Corma, S. Iborra, I. Rodriguez, F. Sanchez, *J. Catal.* **2002**, *211*, 208–215; b) M. J. Climent, A. Corma, S. Iborra, A. Velty, *J. Mol. Catal. A* **2002**, *182–183*, 327–342; c) M. Trilla, R. Pleixats, M. W. C. Man, C. Bied, *Green Chem.* **2009**, *11*, 1815–1820; d) G. Postole, B. Chowdhury, B. Karmakar, K. Pinki, J. Banerji, A. Auroux, *J. Catal.* **2010**, *269*, 110–121; e) C. Yue, A. Maob, Y. Y. Wei, M. J. Lu, *Catal. Commun.* **2008**, *9*, 1571–1574; f) S. L. Hruby, B. H. Shanks, *J. Catal.* **2009**, *263*, 181–188; g) M. Boronat, M. J. Climent, A. Corma, S. Iborra, R. Monton, M. J. Sabater, *Chem. Eur. J.* **2010**, *16*, 1221–1231.
- [6] M. J. Climent, A. Corma, H. Garcia, R. Guil-Lopez, S. Iborra, V. Fornés, *J. Catal.* **2001**, *197*, 385–393.
- [7] T. Welton, *Coord. Chem. Rev.* **2004**, *248*, 2459–2477.
- [8] T. Okino, Y. Hoashi, T. Furukawa, X. Xu, Y. Takemoto, *J. Am. Chem. Soc.* **2005**, *127*, 119–125.
- [9] I. V. Kozhevnikov, *Chem. Rev.* **1998**, *98*, 171–198.
- [10] A. Yoshida, S. Hikichi, N. Mizuno, *J. Organomet. Chem.* **2007**, *692*, 455–459.
- [11] J. Juan-Alcaniz, E. V. Ramos-Fernandez, U. Lafont, J. Gascon, F. Kapteijn, *J. Catal.* **2010**, *269*, 229–241.
- [12] Y. Liu, K. Murata, M. Inaba, *Catal. Commun.* **2005**, *6*, 679–683.
- [13] a) P. G. Rickert, M. R. Antonio, M. A. Firestone, K. Kubatko, T. Szreder, J. F. Wishart, M. L. Dietz, *J. Phys. Chem. B* **2007**, *111*, 4685–4692; b) A. B. Bourlinos, K. Raman, R. Herrera, Q. Zhang, L. A. Archer, E. P. Giannelis, *J. Am. Chem. Soc.* **2004**, *126*, 15358–15359.
- [14] a) Y. Zhang, Y. Shen, J. Yuan, D. Han, Z. Wang, Q. Zhang, L. Niu, *Angew. Chem.* **2006**, *118*, 5999–6002; *Angew. Chem. Int. Ed.* **2006**, *45*, 5867–5870; b) M. Ammann, J. Fransaer, *J. Solid State Chem.*

- 2011**, 184, 818–824; c) C. Petit, T. J. Bandosz, *J. Phys. Chem. C* **2009**, 113, 3800–3809.
- [15] a) W. Liu, H. Tan, W. Chen, Y. Li, E. Wang, *J. Coord. Chem.* **2010**, 63, 1833–1843; b) W. Chen, B. Chen, H. Tan, Y. Li, Y. Wang, E. Wang, *J. Solid State Chem.* **2010**, 183, 310–321; c) P. G. Rickert, M. R. Antonio, M. A. Firestone, K. Kubatko, T. Szreder, J. F. Wishart, M. L. Dietz, *Dalton Trans.* **2007**, 529–531.
- [16] a) S. Luo, J. Li, H. Xu, L. Zhang, J. Cheng, *Org. Lett.* **2007**, 9, 3675–3678; b) J. Li, X. Li, P. Zhou, L. Zhang, S. Luo, J. Cheng, *Eur. J. Org. Chem.* **2009**, 4486–4493.
- [17] a) Y. Leng, J. Wang, D. Zhu, X. Ren, H. Ge and L. Shen, *Angew. Chem.* **2008**, 121, 174–177; *Angew. Chem. Int. Ed.* **2008**, 48, 168–171; b) Y. Leng, J. Wang, D. Zhu, Y. Wu, P. Zhao, *J. Mol. Catal. A* **2009**, 313, 1–6; c) W. Zhang, Y. Leng, P. Zhao, J. Wang, D. Zhu, J. Huang, *Green Chem.* **2011**, 13, 832–834; d) Y. Leng, J. Wang, D. Zhu, M. Zhang, P. Zhao, Z. Long, J. Huang, *Green Chem.* **2011**, 13, 1636–1639; e) P. Zhao, Y. Leng, M. Zhang, J. Wang, Y. Wu, J. Huang, *Chem. Commun.* **2012**, 48, 5721–5723; f) P. Zhao, M. Zhang, Y. Wu, J. Wang, *Ind. Eng. Chem. Res.* **2012**, 51, 6641–6647.
- [18] a) S. A. Patel, S. Sinha, A. N. Mishra, B. V. Kamath, R. N. Ramb, *J. Mol. Catal. A* **2003**, 192, 53–61; b) R. D. Jones, D. A. Summerville, F. Basolo, *Chem. Rev.* **1979**, 79, 139–179; c) E. Hadjoudis, I. M. Mavridis, *Chem. Soc. Rev.* **2004**, 33, 579–588.
- [19] A. Ouadi, B. Gadenne, P. Hesemann, J. J. E. Moreau, I. Billard, C. Gaillard, S. Mekki, G. Moutiers, *Chem. Eur. J.* **2006**, 12, 3074–3081.
- [20] Y. Peng, Y. Cai, G. Song, J. Chen, *Synlett* **2005**, 14, 2147–2150.
- [21] G. R. Rao, T. Rajkumar, B. Varghese, *Solid State Sci.* **2009**, 11, 36–42.
- [22] X. Yan, P. Zhu, J. Fei, J. Li, *Adv. Mater.* **2010**, 22, 1283–1287.
- [23] a) W. Schilf, A. Szady-Chelmieniecka, E. Grech, P. Przybylski, B. Brzezinski, *J. Mol. Struct.* **2002**, 643, 115–121; b) A. Cinarli, D. Gurbuz, A. Tavman, A. S. Birteksoz, *Bull. Chem. Soc. Ethiop.* **2011**, 25, 407–417.
- [24] M. M. Abd-Elzaher, *Appl. Organomet. Chem.* **2004**, 18, 149–155.
- [25] P. M. Rao, A. Wolfson, S. Kababya, S. Vega, M. V. Landau, *J. Catal.* **2005**, 232, 210–215.
- [26] a) A. M. Douvas, K. Yannakopoulou, P. Argitis, *Chem. Mater.* **2010**, 22, 2730–2740; b) L. S. San Felices, P. Vitoria, J. M. Gutierrez-Zorrilla, S. Reinoso, J. Etxebarria, L. Lezama, *Chem. Eur. J.* **2004**, 10, 5138–5146.
- [27] A. Corma, M. Boronat, M. J. Climent, S. Iborra, R. Monton, M. J. Sabater, *Phys. Chem. Chem. Phys.* **2011**, 13, 17255–17261.
- [28] K. Ambroziaka, Z. Rozwadowskia, T. Dziembowska, B. Bieg, *J. Mol. Struct.* **2002**, 615, 109–120.
- [29] J. D. Bass, A. Solovyov, A. J. Pascall, A. Katz, *J. Am. Chem. Soc.* **2006**, 128, 3737–3747.
- [30] I. Rodriguez, G. Sastre, A. Corma, S. Iborra, *J. Catal.* **1999**, 183, 14–23.
- [31] A. R. Gholap, K. Venkatesan, T. Daniel, R. J. Lahoti, K. V. Srinivasan, *Green Chem.* **2003**, 5, 693–696.
- [32] a) R. Wirz, D. Ferri, A. Baiker, *Langmuir* **2006**, 22, 3698–3706; b) A. Corma, V. Fornes, R. M. Martin-Aranda, H. Garcia, J. Primo, *Appl. Catal. A* **1990**, 59, 237–248.
- [33] M. Misono, *Chem. Commun.* **2001**, 1141–1152.
- [34] E. D. Bates, R. D. Mayton, I. Ntai, J. H. Davis, *J. Am. Chem. Soc.* **2002**, 124, 926–927.
- [35] a) J. Etteguai, R. Neumann, *J. Am. Chem. Soc.* **2009**, 131, 4–5; b) Z. Fei, D. Zhao, T. J. Geldbach, R. Scopelliti, P. J. Dyson, *Eur. J. Inorg. Chem.* **2005**, 860–865.

Received: April 19, 2012  
Published online: August 21, 2012